JOURNAL OF AGRICULTURAL AND FOOD CHEMISTRY

Proteome-Level Investigation of *Brassica carinata*-Derived Resistance to *Leptosphaeria maculans*

BABU SUBRAMANIAN, VIPAN K. BANSAL, AND NAT N. V. KAV*

Department of Agricultural, Food and Nutritional Science, University of Alberta, Edmonton, Alberta T6G 2P5, Canada

Plants resistant to the fungal pathogen *Leptosphaeria maculans* were generated by an interspecific cross between the highly susceptible *Brassica napus* (canola) and the highly resistant *Brassica carinata*. Changes in the leaf protein profiles of these lines were investigated in order to understand the biochemical basis for the observed resistance. Two-dimensional electrophoresis followed by tandem mass spectrometry led to the identification of proteins unique to the susceptible (5 proteins) and resistant genotypes (7 proteins) as well those that were differentially expressed in the resistant genotype 48 h after challenge with the pathogen (28 proteins). Proteins identified as being unique in the resistant plant material included superoxide dismutase, nitrate reductase, and carbonic anhydrase. Photosynthetic enzymes (fructose bisphosphate aldolase, triose phosphate isomerase, sedoheptulose bisphosphatase), dehydroascorbate reductase, peroxiredoxin, malate dehydrogenase, glutamine synthetase, *N*-glyceraldehyde-2-phosphotransferase, and peptidyl-prolyl *cis*−*trans* isomerase were observed to be elevated in the resistant genotype upon pathogen challenge. Increased levels of the antioxidant enzyme superoxide dismutase were further validated and supported by spectrophotometric and in-gel activity assays. Other proteins identified in this study such as nitrate reductase and peptidylprolyl isomerase have not been previously described in this plant−pathogen system, and their potential involvement in an incompatible interaction is discussed.

KEYWORDS: ***Brassica napus*; canola; *Leptosphaeria maculans*; mass spectrometry; proteomics; peptidylprolyl isomerase; superoxide dismutase**

INTRODUCTION

Stem canker or "blackleg" caused by *Leptosphaeria maculans* (Desm.) ces. & de Not. [anamorph: *Phoma lingam* (Tode ex Fr.)] is a devastating fungal disease of oilseed brassica crops worldwide. Consequently, a detailed understanding of the resistance mechanisms and the development of resistant plants through conventional breeding as well as by genetic engineering is highly desirable. Although differential host responses contributing to the possible mechanisms of resistance have been described, little is known about the molecular details underlying resistance to this pathogen. Investigations on resistant traits have demonstrated that adult plant resistance may be controlled by several genes, whereas seedling resistance is often described as a single-gene trait (*1*). Genetic evidence for a gene-for-gene relationship has been established (*2*); however, in some Australian isolates of *L. maculans*, seedling disease and stem canker were found to be confined to the same locus in the fungal genome (*3*).

The genetic basis of resistance to *L. maculans* is, to a large extent, unclear even though several biochemical and molecular studies toward understanding the defense responses of host plants to *L. maculans* infection have revealed hypersensitive responses, lignin and callose deposition and accumulation of pectin-like substances (*4*, *5*), induction of pathogenesis-related (PR) proteins (*6*), phytoalexins (*7*), systemic acquired resistance (*8*), and several expressed sequence tags (ESTs) of unknown function (*9*). A recent study on the incompatible *Arabidopsis*−*L. maculans* pathosystem revealed that the resistance may be partially due to the phytoalexin, camalexin, whereas it appeared to be independent of salicylic acid, ethylene, and jasmonic acid signaling (*1*). These results suggest that the defense response to *L. maculans* might involve complex, multiple, and previously uncharacterized pathways.

A high degree of resistance to blackleg in all plant parts is found in species such as *Brassica nigra*, *Brassica juncea*, and *Brassica carinata*, which could potentially be used to breed for disease resistance (*10*, *11*). However, there are alarming reports describing isolates of *L. maculans* that are virulent against *B. nigra* and *B. juncea* from both Australia and France (*12*, *13*), necessitating the quick identification of novel sources of resistance to rapidly evolving races of *L. maculans* in order to benefit canola breeding programs. *B. carinata* is an amphidiploid member of the cruciferous plant family and, as mentioned previously, the resistance of this species to blackleg as well as other devastating diseases of canola caused by *Alternaria*

* Corresponding author [telephone (780) 492-7584; fax (780) 492-4265; e-mail nat@ualberta.ca].

10.1021/jf048922z CCC: $30.25
Published on Web 12/29/2004

brassicae and *Albugo candida* makes it desirable as a potential source of new genes for resistance to these diseases.

Utilizing *B. carinata* as a source of resistance, the canola breeding program at the University of Alberta has developed lines of canola that have demonstrated resistance to the PG2 group of *L. maculans* (prevalent in Canada) at both cotyledonary and adult stages. We have compared proteome-level differences between resistant and susceptible genotypes as well as the changes that occur in these genotypes in response to the pathogen. Several proteins that were unique to the genotypes as well as those that were differentially expressed in the resistant genotype 48 h after challenge with the pathogen were identified using two-dimensional electrophoresis followed by tandem mass spectrometry (MS). The potential role of these proteins in this host−pathogen interaction as well as in potentially mediating the observed resistance is discussed.

MATERIALS AND METHODS

Plant Material, Fungal Culture, and Chemicals. Seeds (BC_2F_6) from blackleg-susceptible (02-17034−12) and-resistant (02-17044-9) lines were obtained from the canola breeding program at the University of Alberta. These lines were derived from a cross between *B. napus* cv. Westar (highly susceptible to blackleg) and *B. carinata* (highly resistant) and subsequent backcrosses with *B. napus*. A highly virulent PG2 isolate of *L. maculans* (77-33) was provided by Dr. J. P. Tewari, Department of Agricultural, Food and Nutritional Science at the University of Alberta.

Plant and Fungal Growth, Inoculation, Evaluation of Disease, and Sampling. Seeds of each genotype were sown in plastic inserts (2.5 × 2 in.; two seeds per insert) containing Metro Mix 290 (Grace Horticultural Products, Ajax, ON, Canada) consisting of vermiculite and sphagnum peat moss. Plants were allowed to grow in the greenhouse (22 °C day/18 °C night; 16 h photoperiod) for 2 weeks and, 24 h prior to inoculation, were transferred to a humidity chamber [100% relative humidity (RH)]. True leaves were wounded using a pipet tip and inoculated with 10 μL of spore suspension (10^7 spores/mL) or sterile water (control). After 1 h, the plants were returned to the humidity chamber for an additional 24 h, after which they were transferred to the greenhouse and watered uniformly every 48 h. True leaves (inoculated and newly formed) were collected from 10 plants of each treatment at 48 h postinoculation for proteome analysis. Disease severity was scored 15 days postinoculation on a total of 12 plants/treatment with three replications per treatment (i.e., 4 plants per replication) using a scale of 0−4; 0 indicates no visible expression of disease; 1, necrotrophic hypersensitive response around the wound site; 2, gray-green tissue collapse with distinct margin; 3, gray-green tissue collapse with diffused margin; and 4, 1−4 cm of tissue around the wound collapsed with pycnidia formation, and mean disease severity was calculated using the formula of Bansal et al. (*14*).

Statistical Analysis. Disease severity was analyzed using the mixed model procedure of the Statistical Analysis System (SAS). An arcsine transformation was used to meet normality assumptions. The design was a 2 × 2 factorial with genotype (susceptible and resistant) and inoculation (uninoculated and inoculated) considered as fixed effects and replications as blocks. The block was included as a random effect in the model. Least-squares means and standard errors were obtained for fixed effects and interaction of genotype and inoculation.

Protein Extraction for Two-Dimensional Gel Electrophoresis. Pooled leaf tissue from 10 plants at 48 h postinoculation as well as control plants was flash frozen in liquid nitrogen and ground to a fine powder. Tissue powder (200 mg) was resuspended in 1 mL of 10% (w/v) trichloroacetic acid (TCA) in acetone containing 0.07% dithiothreitol (DTT). This extract was incubated at −20 °C for 1 h, after which it was centrifuged at 14000 rpm for 15 min at 4 °C, and the pellet was resuspended in 1 mL of ice-cold acetone containing 0.07% DTT and centrifuged as above. The pellet was washed four more times with ice-cold acetone containing 0.07% DTT, air-dried at room temperature for 10 min, and resuspended in 500 μL of rehydration/sample buffer (Bio-Rad, Mississauga, ON, Canada) and incubated overnight at 4 °C, after which the sample was vortexed and centrifuged as previously described. The supernatant was transferred to a fresh tube, protein concentration was determined using a modified Bradford assay (Bio-Rad), and all samples were stored at −20 °C until two-dimensional gel electrophoresis was performed.

Two-Dimensional Electrophoresis. A solution containing 100 or 150 μg of protein in a 125 μL total volume was used for passive rehydration of 7 cm, pH 4−7 linear IPG strips (Bio-Rad), and for the longer 17 cm (pH 4−7, linear) strips, 300 μg of protein in 300 μL of rehydration buffer was used. Isoelectric focusing (IEF) was performed using a Bio-Rad Protean IEF unit programmed to provide an optimum, maximum field strength of 600 V/cm and a 50 μA limit/IPG strip. Initially, a low voltage of 250 V was applied for 15 min to remove salt ions and charged contaminants after which a linear ramping step was applied to reach 4000 V in 2 h (to 10000 V in 3 h for 17 cm strips) at which point focusing took place at 4000 V for 20000 Vh (at 10000 V for 60000 Vh for 17 cm strips). After IEF, strips were held at 500 V. When focusing was complete, the strips were removed from the focusing tray and placed gel side up in a reswelling tray for storage at −20 °C overnight. Prior to second-dimension sodium dodecyl sulfate−polyacrylamide gel electrophoresis (SDS-PAGE), the focused proteins in the strips were equilibrated to reduce and alkylate proteins, as previously described (*15*). The equilibrated 7 cm strips were placed on top of 13% polyacrylamide gels (7 × 8 cm, 1 mm thickness), and electrophoresis was carried out in a Bio-Rad Mini Protean 3 system at a constant voltage (160 V). Electrophoresis was terminated 15 min after the dye front had reached the bottom of the gel. For the 17 cm IPG strips, second-dimension electrophoresis was carried out on 13% polyacrylamide gels (20 × 20 cm, 1 mm thickness) using a Protean II xi system (Bio-Rad) at 75 V overnight followed by 150 V for an additional 5 h. Gels were stained either with silver using the Silver Stain Plus kit (Bio-Rad) or with Coomassie Brilliant Blue R250 (Aldrich, Oakville, Canada) and scanned using the GS-800 calibrated densitometer (Bio-Rad).

Image Analysis. Images of the two-dimensional gels were analyzed using the automated spot detection matching tool and spot identification wizard of the PDQuest software (Bio-Rad). After the spots were automatically matched, manual validation and addition/removal of spots was performed to include those that were missed and to eliminate artifacts. After all of the spots were matched, those that were unique to either genotype and those that showed altered levels in response to pathogen infection were quantified using the spot quantification tool of the PDQuest software. The density of a particular spot from control (uninoculated) gels was equated to one, and the fold up- or down-regulation 48 h after pathogen inoculation was calculated and expressed as a ratio. Protein extracts prepared from each of three independent inoculation experiments were used for two-dimensional electrophoresis (three gels per treatment). Spots that showed reproducible differences in all three gels were subjected to ESI-Q-TOF-MS/MS analysis as previously described (*15*).

Superoxide Dismutase (SOD) Activity. SOD activity was assayed as described (*16*) and involved the determination of its ability to inhibit the photochemical reduction of nitro blue tetrazolium (NBT). Leaf tissue (0.1 g) was homogenized in extraction buffer (50 mM HEPES containing 0.1 mM EDTA, pH 7.6). The final assay mixture (1 mL) contained 50 mM HEPES (pH 7.6), 50 mM sodium carbonate (pH 10.4), 13 mM methionine, 0.025% Triton X-100, 75 μM NBT, 2 μM riboflavin, and 100 μL of leaf extract. Tubes were mixed, and the reaction was initiated by placing the tubes under a 40 W fluorescent lamp for 30 min and terminated by switching the lamp off. Identical, nonilluminated samples served as blanks, and tubes containing only the assay mixture (without enzyme extract) were also illuminated in parallel with the sample tubes to determine the maximum reduction of NBT. The absorbance of each sample was determined at 560 nm and was deducted from the maximum values obtained with the samples without the plant extracts, divided by the maximum absorbance, and multiplied by 100 to obtain the percent inhibition of NBT photoreduction (*17*).

In-Gel Analysis of SOD Isozymes. SOD isozymes were analyzed on native polyacrylamide gels as described (*18*). Briefly, the leaf tissue (0.1 g) was extracted in 100 mM potassium phosphate buffer (pH 7.8)

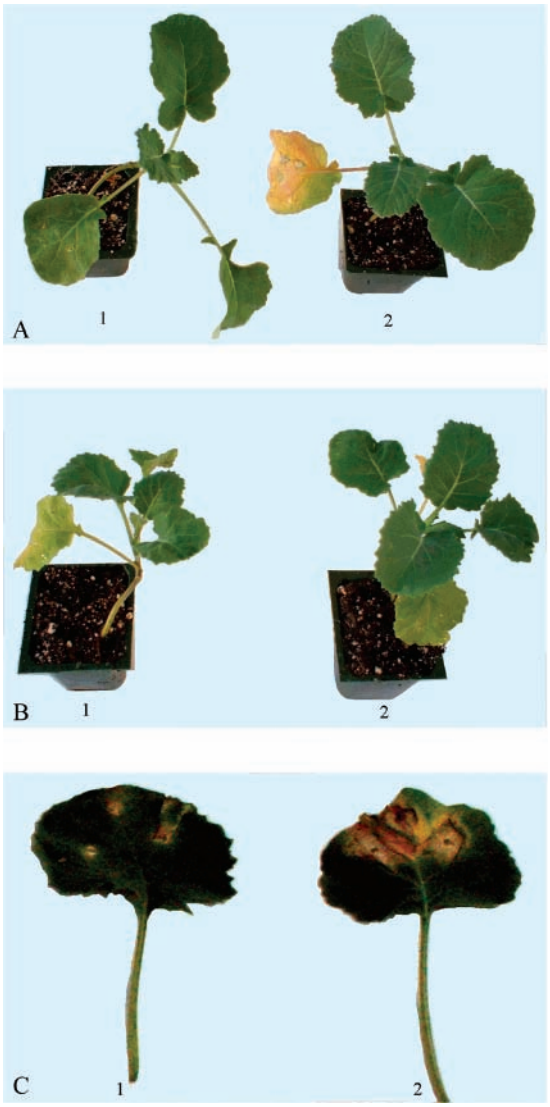

Figure 1. Symptoms expressed by blackleg-susceptible and-resistant genotypes: (**A**) susceptible genotype [(**1**) uninoculated plant; (**2**) inoculated plant]; (**B**) resistant genotype [(**1**) uninoculated plant; (**2**) inoculated plant]. (**C**) Symptoms expressed by leaves: (**1**) leaf from a resistant inoculated plant; (**2**) leaf from a susceptible inoculated plant.

containing 0.5% Tween 20 and the extracted protein quantified using a modified Bradford method using bovine serum albumin (BSA) as standard (Bio-Rad). Protein samples (100 μg) were loaded on non-denaturing polyacrylamide gels (4% stacking and 15% separating), and electrophoresis was carried out at 100 V at 4 °C. Gels were incubated in 100 mL of 50 mM potassium phosphate buffer (pH 7.8) containing 200 μL of *N*,*N*,*N*′,*N*′-tetramethylethylenediamine (TEMED), 1 mL of 10 mM ethylenediaminetetraacetic acid (EDTA), 150 mg of riboflavin, and 15 mg of NBT. After incubation for 30 min in dark, the gels were submerged in the above phosphate buffer and illuminated under 40 W fluorescent bulbs until maximal contrast between clearer SOD bands against a blue background (~5 min) was attained. The gels were further destained in water overnight, and the experiment was repeated twice.

RESULTS AND DISCUSSION

Disease Severity and Symptoms. Appearance of susceptible and resistant plants 2 weeks after pathogen challenge is shown in panels **A** and **B**, respectively, of **Figure 1**. Susceptible plants exhibited symptoms such as necrosis around the inoculated spot with irregular margin and formation of pycnidia in the necrotic region (**Figure 1C**). In some plants, the necrosis extended along the midrib to the petioles, and in others, symptoms of blackleg were visible. However, the resistant plants expressed a hypersensitive response where the necrosis was limited to the inoculation spot (**Figure 1C**). A significant difference in the severity of the disease, calculated on the basis of scoring the intensity, between the two genotypes was observed with the susceptible and resistant plants recording mean disease severities of 69.8 and 19.1%, respectively (**Table 1**).

Table 1. Reaction of *Brassica* Genotypes to Artificial Inoculation of *L. maculans*

genotype and treatment[a]	disease severity[b] (%)
SG	
uninoculated	
inoculated	69.79 ± 3.58
RG	
uninoculated	
inoculated	19.09 ± 3.58

[a] SG, susceptible genotype; RG, resistant genotype. [b] Values are the mean of three experiments with three replications each. Values following ± symbols indicate standard error of mean.

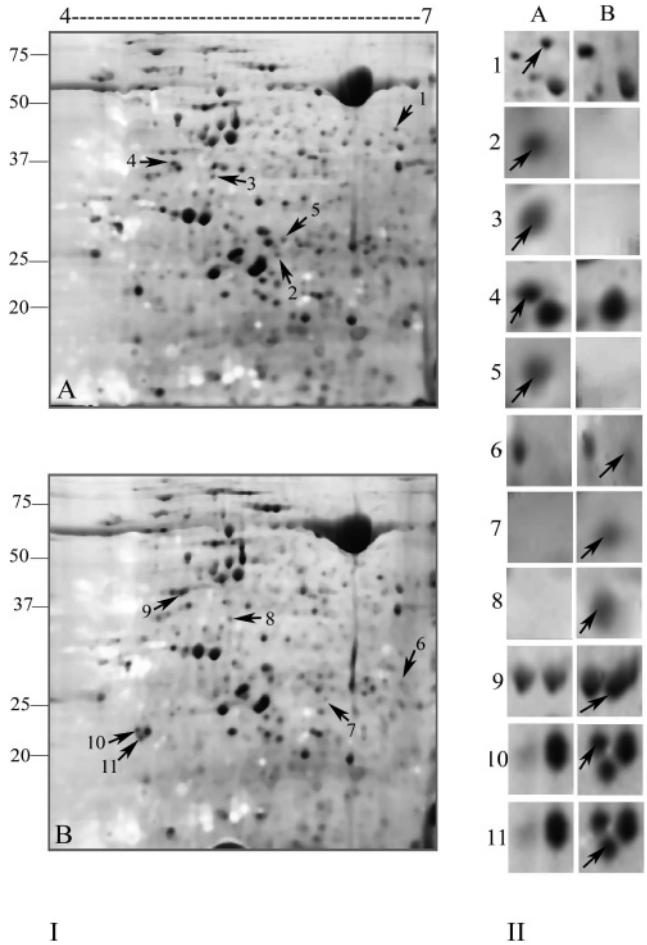

Figure 2. (**I**) Silver-stained two-dimensional gels of leaf proteins from uninoculated susceptible and resistant genotypes: (**A**) susceptible, uninoculated; (**B**) resistant, uninoculated. Proteins selected for mass spectrometry are indicated by arrows and numbers. Numbers on the left indicate molecular mass in kilodaltons. (**II**) Enlarged regions of gels showing the genotype-specific spots.

Comparison of Leaf Proteomes. The gels of total leaf proteins extracted from pooled, uninoculated susceptible and resistant plants subjected to two-dimensional electrophoresis are shown in **Figure 2** (silver stained) and **Figure 3** (Coomassie

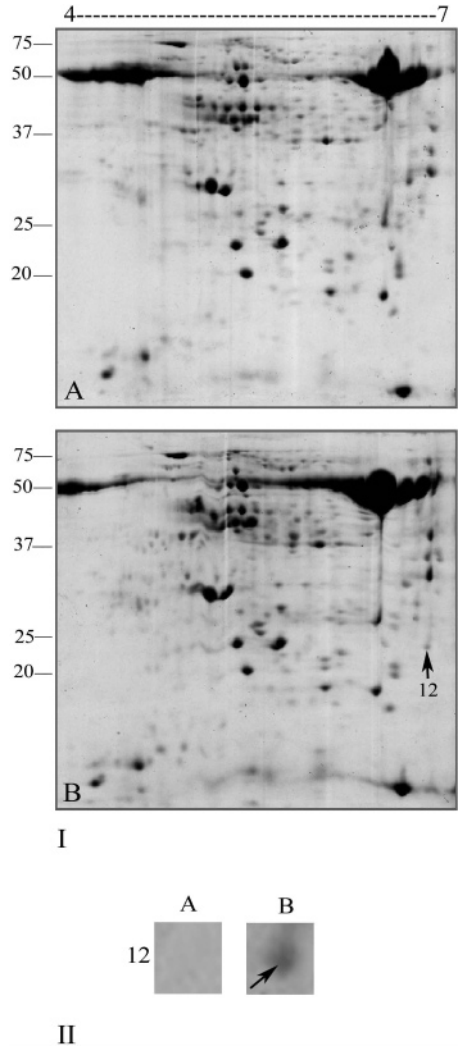

Figure 3. (**I**) Coomassie blue stained two-dimensional electrophoresis gels of leaf proteins from uninoculated susceptible and resistant genotypes: (**A**) susceptible, uninoculated; (**B**) resistant, uninoculated. Proteins selected for mass spectrometry are indicated by arrow and number. Numbers on the left indicate molecular mass in kilodaltons. (**II**) Enlarged regions of gels showing the spot.

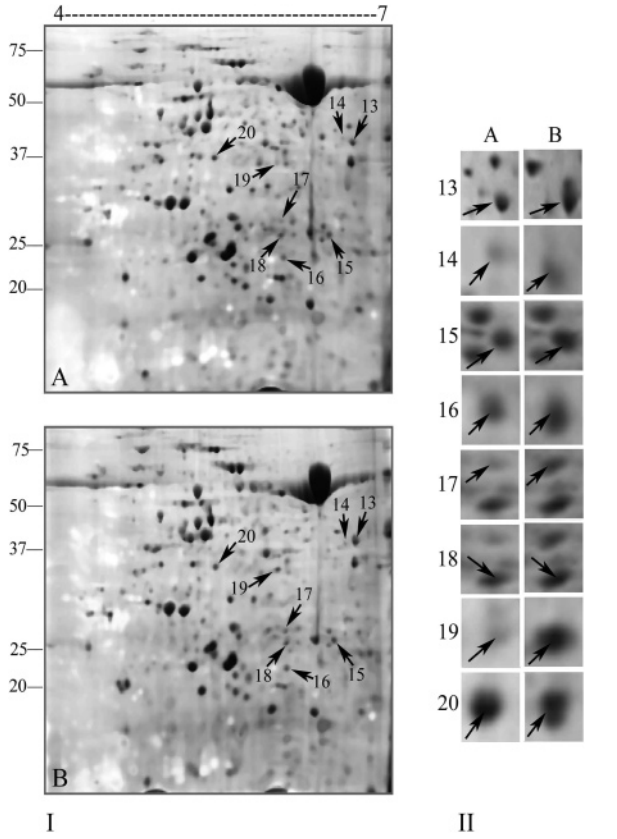

Figure 4. (**I**) Silver-stained two-dimensional electrophoresis gels of leaf proteins from susceptible and resistant genotypes 48 h post-inoculation: (**A**) susceptible, inoculated; (**B**) resistant, inoculated. Proteins selected for mass spectrometry are indicated by arrows and numbers. Numbers on the left indicate molecular mass in kilodaltons. (**II**) Enlarged regions of gels showing the differently expressed spots.

blue stained). The identities of unique spots established by MS are listed in **Table 2**. Apart from identifying proteins unique to the susceptible and resistant genotypes, we were also interested in identifying proteins that increased in the resistant genotype 48 h after challenge with the pathogen in order to further probe the biochemical basis for the observed resistance phenotype. Representative images of these gels stained with silver or Coomassie blue are shown in **Figures 4** and **5**, respectively. Eight spots that showed increase in intensities in the resistant genotype in response to the pathogen were visible on mini gels stained with silver (**Figure 4**), 13 spots were visible on mini gels stained with Coomassie blue (**Figure 5**), and 7 additional spots were visible on larger format gels stained with silver (**Figure 6**).

The relative levels of these proteins are expressed as a ratio of the fold increase in the resistant plants compared to the susceptible plants after challenge with the pathogen and are the mean values obtained from three independent inoculation experiments (**Table 3**). The identities of the proteins that showed pathogen-induced increase of at least 1.5-fold in the resistant plants over the susceptible plants are presented in **Table 3**. The majority of proteins identified in this study included antioxidants and related enzymes, enzymes involved in CO_2 fixation and regeneration, photorespiratory enzymes, and proteins involved in nitrogen metabolism, as well as some with as of yet unknown function. Some of the leaf proteins identified in this study may have potential roles in blackleg disease resistance, and these are grouped according to their known functions and discussed below.

Antioxidants and Related Enzymes. Under stress conditions, such as pathogen infection, which induce an overproduction of reactive oxygen species (ROS) in cells, the ability of plants to increase the activity of ROS-detoxifying enzymes or the biosynthesis or regeneration of antioxidant metabolites has a crucial role in ameliorating the stress (*19*). ROS-detoxifying enzymes such as SOD catalyze the dismutation of ROS such as O_2^- to H_2O_2, thus ameliorating their toxic effects. Alternatively, ROS can act directly against plant pathogens and kill the microorganism. However, when ROS levels increase above a threshold, deleterious effects such as necrosis of plant cells occur. Therefore, excess ROS are scavenged by enzymes and redox metabolites. A unique protein (spot 12; **Figure 3**) was identified as SOD in uninoculated resistant plants, which suggest that the resistant plants may possess additional SOD isozymes that are constitutively expressed. These SOD isozymes may aid in detoxifying the O_2^- generated during pathogen attack and may be crucial in combating the deleterious effects brought about by pathogen infection.

Additional support for the potential role of cellular antioxidant status in the resistance mechanism comes from the identification of another protein, dehydroascorbate reductase, the levels of

Table 2. Summary of Unique Proteins Identified in Susceptible and Resistant Genotypes

spot	Figure	identity	peptides matched	accession no.	M_r/p*I*
			Susceptible Genotype		
1	**2**	fructose-bisphosphate aldolase	ALQQSTLK GILAADESTGTIGK	gi|113622 *Oryza sativa*	39185/8.50
2	**2**	thylakoid luminal 20 kDa protein	IGDQTYYK	gi|15228983 *Arabidopsis thaliana*	28726/9.30
3	**2**	mutator-like trasposase	VDSTWLSER	gi|14719322 *O. sativa*	84299/8.25
4	**2**	glutamine synthetase	AAEIFSNK EDGGFEVIK	gi|6966930 *Brassica napus*	47889/6.37
5	**2**	triose-phosphate isomerase	CNGTAEEVK VAYALAQGLK EAGSTMDVVAAQTK NVSADVAATTR	gi|11270444 *A. thaliana*	27366/5.24
			Resistant Genotype		
6	**2**	carbonic anhydrase	YMVFSCADSR	gi|7436816 *O. sativa*	29585/8.41
7	**2**	thylakoid luminal 20 kDa protein	IGDQTYYK	gi|15228983 *A. thaliana*	28726/9.30
8	**2**	cyclin, B-type	KATVKPNPEDIIEISPDTQEK SKAACGLSK VHDYMDSQPEINDRMR MRAVLIDWLVEVHQK FELNPETLYLTINIVDRYLAVK SYTHDQVLAMEK EILGQLEWYLTVPTPYVFLAR TPFWNETLKLHTGFSESQLIECAR LHTGFSESQLIECARLLVSYQSAAATHK MVVVGCQRCHMYVMVTEADPR	gi|7438486 *Nicotiana tabacum*	53164/9.08
9	**2**	sedoheptulose-bisphosphatase precursor	TTYVLAVK ATFDNSEYSK GIFTNVTSPTAK FEETLYGTSR	gi|15228194 *A. thaliana*	42787/6.17
10	**2**	nitrate reductase	LTGKHPLNCEPPLAR LMHHGFITPAPLHYVR NHGAVPRGDWATWTVEVTGLVR KEQNMVQQTVGFNWGAAGVSTSVWR EQNMVQQTVGFNWGAAGVSTSVWR RCGIVPR VIIPGCIGGR RIIVTPAESDNYYHFK GYTMKGYAYSGGGK GYAYSGGGK VTRVEVTLDGGETWLVCHLDHPEKPNK VNVCRPHK GEIGLVFEHPTQPGNQPGGWMARQK QKHLETAEAAAPGLK STSTPFMNTTDVGK QFTMSEVR HASQESAWIAVHGHVYDCTKFLK DHPGGADSILINAGTDCTEEFDAIHSDK ALLDTYR RPEEGWK	gi|5020385 *Zea mays*	102539/6.37
11	**2**	hypothetical protein	EFMFQR LRVAAGQLPDPVVK SGNIINVLEIGQAVK GESLAAPATSSTRCR GSCSRCWLTVVCGGVR VAAGQLPDPVVKEGDEQYR SGNIINVLEIGQAVKEFMFQR EFMFQRHEMVHTVGVWPRPSTSK ICCHIFPACGPVKECGAQTGHVFSR	gi|21450451 *O. sativa*	32145/5.41
12	**3**	superoxide dismutase	AYVDNLKK QVLGSELEGK TFMNNLVSWEAVSSR QTLEFHWGK	gi|3114705 *Raphanus sativus*	23791/5.96

which increased in the resistant plants upon pathogen challenge (spot 18; **Table 3**; **Figure 4**). Dehydroascorbate reductase is another enzyme involved in the protection of cellular components against oxidative stress. Superoxide anions are effectively removed by SOD, and the H_2O_2 that is generated is detoxified to water by ascorbate peroxidase, leading to the production of monodehydroascorbate [MDA; (*20*)]. MDA is rapidly returned to the ascorbate pool by monodehydroascorbate reductase (MDAR); however, when MDA levels are high, as would be expected under oxidative stress including pathogen attack, they disproportionate to ascorbate and dehydroascorbate (DHA). The activity of dehydroascorbate reductase (DHAR) recycles dehydroascorbate to ascorbate, and an increase in DHAR activity as well as the accumulation of DHA has been frequently implied as biochemical indicators of oxidative stress in plant metabolism (*21*). Increased SOD could potentially result in increased levels of H_2O_2, leading to increased levels of DHA due to the inability of MDAR to reduce all of the MDA formed. In resistant genotype (RG) plants, the observed increase in DHAR may reduce DHA to ascorbic acid and help maintain ascorbate levels, thereby affording protection from oxidative stress. This hypothesis is supported by a report in maize, where increased DHAR

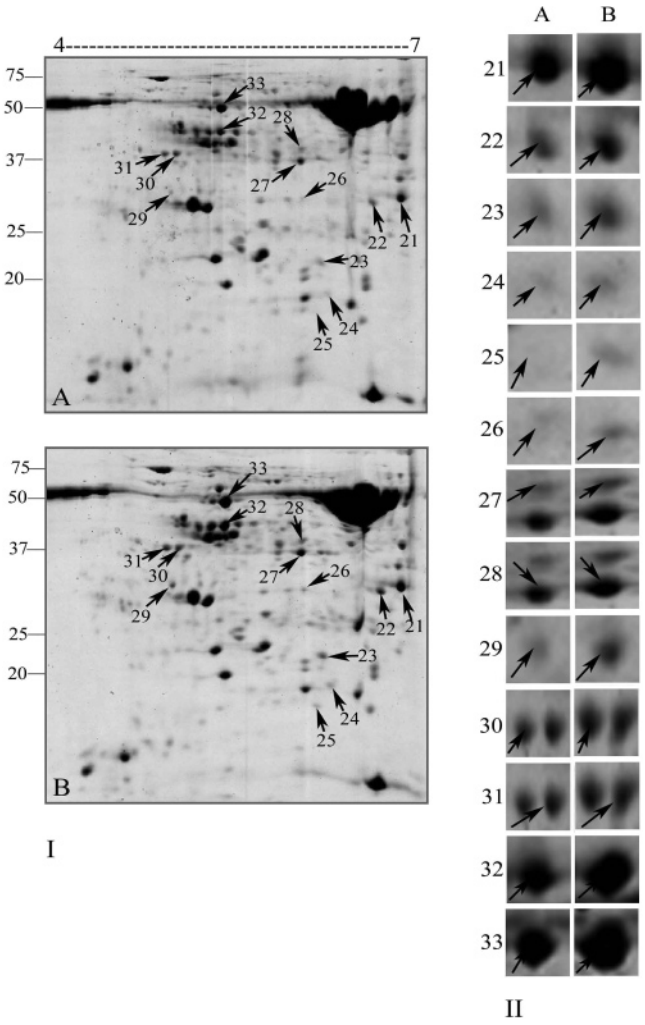

Figure 5. (**I**) Coomassie blue stained two-dimensional electrophoresis gels of leaf proteins from susceptible and resistant genotypes 48 h post-inoculation: (**A**) susceptible, inoculated; (**B**) resistant, inoculated. Proteins selected for mass spectrometry are indicated by arrows and numbers. Numbers on the left indicate molecular mass in kilodaltons. (**II**) Enlarged regions of gels showing the differently expressed spots.

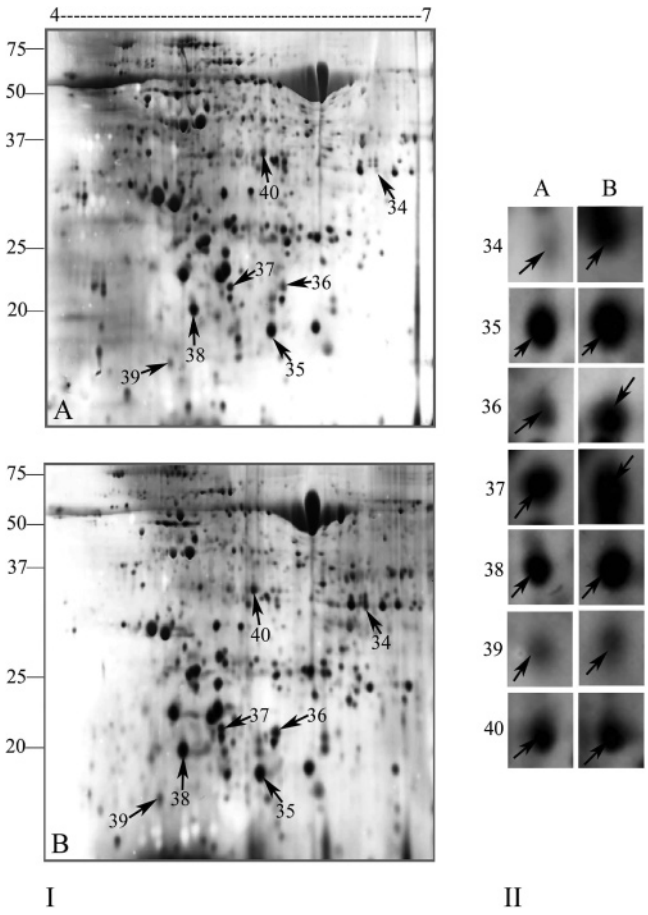

Figure 6. (**I**) Silver-stained two-dimensional electrophoresis large format gels of leaf proteins from resistant genotype uninoculated and inoculated 48 h post-inoculation: (**A**) resistant, uninoculated; (**B**) resistant, inoculated. Proteins selected for mass spectrometry are indicated by arrows and numbers. Numbers on the left indicate molecular mass in kilodaltons. (**II**) Enlarged regions of gels showing the differently expressed spots.

activities were reported in transgenic plants overexpressing Mn-SOD (*22*). In our current study, the increase in dehydroascorbate reductase in the resistant genotype upon challenge with the pathogen is not as prominent as some of the other protein spots (**Table 3**). The precise role of this enzyme in this host−pathogen interaction as well as in mediating resistance to this pathogen needs to be further characterized.

Peroxiredoxin (spot 39; **Table 3**; **Figure 6**), a protein involved in maintaining antioxidant status, was found to be elevated 8-fold in the resistant genotype after 48 h of pathogen challenge (**Table 3**). Peroxiredoxins are able to protect DNA, membranes, and certain enzymes in vitro against damage by thiol or oxygen radicals and to remove H_2O_2, alkyl hydroperoxides, and hydroxyl radicals (*23, 24*). It has been reported that suppression of peroxiredoxin in *Arabidopsis* enhances activities of enzymes associated with ascorbate metabolism but not glutathione metabolism, suggesting a link between peroxiredoxin levels and ascorbate metabolism (*25*). Our current data have revealed elevated levels of dehydroascorbate reductase and peroxiredoxin in the resistant genotype (**Table 3**), which may be indicative of a role for proteins associated with cellular antioxidant status in the incompatible *Brassica*−*Leptosphaeria* interaction characterized in this study.

Proteins Involved in CO_2 Fixation and Related Pathways. The 13 reactions of the Calvin cycle are catalyzed by 11 different enzymes that utilize the products of the light reactions of photosynthesis, to fix CO_2 into carbon skeletons for starch and sucrose biosynthesis (*26*, *27*). One of these enzymes, sedoheptulose bisphosphatase (SBPase), functions in the regenerative phase of the Calvin cycle and aids in the regeneration of ribulose bisphosphate, which is used for another round of CO_2 fixation. In the present study, one protein from silver-stained gels (spot 9; **Table 2**; **Figure 2**) and two proteins from Coomassie-stained gels (spots 30 and 31; **Table 3**; **Figure 5**) were identified as SBPase. Among the three proteins, one (spot 9) is unique to the resistant plants and the other two (spots 30 and 31) are present in both genotypes but are up-regulated in resistant plants and are further increased after pathogen challenge (**Figure 5**; **Table 3**). Peptides from all three spots (9, 30, and 31) exhibited homology to a single SBPase from *Arabidopsis*, but the peptides that were identified differed slightly (**Tables 2** and **3**). Another important enzyme that is important for the activity of the Calvin cycle is triose phosphate isomerase (TPI). A spot identified as TPI (spot 17) was up-regulated in resistant plants ∼3-fold after 48 h of pathogen challenge (**Table 3**; **Figure 4**).

In addition to SBPase and TPI other Calvin cycle enzymes that were identified include fructose bisphosphate aldolase (FBPase). Protein spots with homologies to FBPase included spot 1, which was unique to the susceptible genotype (**Table**

Table 3. Summary of Differentially Regulated Proteins Identified in Susceptible and Resistant Genotypes

spot	Figure	quantity ratio of spots[a], sus vs res inoculated	identity	peptides matched	accession no.	M_r/p*I*
13	**4**	1:1.62	malate dehydrogenase	SQAAALEK LSVPVSDVK EFAPSIPEK	gi|15219721 *A. thaliana*	35890/6.11
14	**4**	1:2.13	putative cytochrome P450	EWAKPMEFIPER	gi|15292873 *A. thaliana*	71726/7.65
15	**4**	1:2.67	AT5g41020/MEE6_9	VDSEETGEEFISEHSSMKDK DGFTGEDMEITGRESEK KPIRIDSEAVDAVK ESGGDVIENTESSKVSDR	gi|10140672 *A. thaliana*	57952/7.54
16	**4**	1:1.57	rubisco large subunit	LNYYTPEYETK	gi|131907 *Angiopteris lygodiifolia*	53138/5.91
17	**4**	1:2.95	triose-phosphate isomerase	CNGTAEEVKK VAYALAQGLK EAGSTMDVVAAQTK NVSADVAATTR IIYGGSVNGGNCK	gi|11270444 *A. thaliana*	27366/5.24
18	**4**	1:1.52	dehydroascorbate reductase	VLLTLEEK YPEPSLK TPPEFASVGSK	gi|15222163 *A. thaliana*	23506/5.79
19	**4**	1:3.41	hypothetical protein H1flk	VSEEGTITEK	gi|99733 *A. thaliana*	59483/6.11
20	**4**	1:1.76	unknown protein	AEDTGELTEK VEEALER	gi|21595827 *A. thaliana*	37661/8.13
21	**5**	1:3.04	rubisco large subunit	AVYECLR AMHAVIDR SQAETGEIK VALEACVQAR DNGLLLHIHR DLAVEGNEIIR ESTLGFVDLLR FLFCAEAIYK EITFNFPTIDK LNYYTPEYETK LSGGDHVHAGTVVGK DDENVNSQPFMR LEGDRESTLGFVDLLR GHYLNATAGTCEEMMKGGLDFTKDD ENVNSQPFMR	gi|1346967 *B. napus*	53436/5.88
22	**5**	1:8.64	rubisco large subunit	AVYECLR AMHAVIDR SQAETGEIK DTDILAAFR VALEACVQAR DLAVEGNEIIR ESTLGFVDLLR LNYYTPEYETK LSGGDHVHAGTVVGK DDENVNSQPFMR EITFNFPTIDKLDGQD ESTLGFVDLLRDDYVEK GGLDFTKDDENVNSQPFMR	gi|1346967 *B. napus*	53436/5.88
23	**5**	1:2.52	rubisco large subunit	DTDILAAFR VALEACVQAR ESTLGFVDLLR FLFCAEAIYK EITFNFPTIDK LNYYTPEYETK TFQGPPHGIQVER	gi|1346967 *B. napus*	53436/5.88
24	**5**	1:3.20	rubisco large subunit	VALEACVQAR DLAVEGNEIIR ESTLGFVDLLR FLFCAEAIYK LSGGDHVHAGTVVGK EITFNFPTIDKLDGQD	gi|1346967 *B. napus*	53436/5.88
25	**5**	1:5.27	cyclophilin	FEDENFTLK	gi|3777556 *Griffithsia japonica*	17471/7.68
26	**5**	1:2.30	rubisco large subunit	DLAVEGNEIIR ESTLGFVDLLR	gi|1346967 *B. napus*	53436/5.88
27	**5**	1:1.84	fructose-bisphosphate aldolase	ANSLAQLGK ALQNTCLK TAAYYQQGAR YTGEGESEEAK ATPEQVAAYTLK LDSIGLENTEANR TVVSIPNGPSALAVK	gi|18420348 *A. thaliana*	43132/6.78

Table 3 (Continued)

spot	Figure	quantity ratio of spots[a], sus vs res inoculated	identity	peptides matched	accession no.	M_r/p*I*
27	**5**	1:1.84	fructose-bisphosphate aldolase	GILAMDESNATCGK MVDVLVEQNIVPGIK GLVPLVGSNNESWCQGLDGLSSR YAAISQDSGLVPIVEPEILLDGEHDIDR	gi|18420348 *A. thaliana*	43132/6.78
28	**5**	1:1.77	AT4g38970/F19H22_70	ANSLAQLGK TAAYYQQGAR AASSYADELVK ATPEQVAAYTLK TVVSIPNGPSALAVK GILAMDESNATCGK YAAISQDSGLVPIVEPEILLDGEHDIDR	gi|16226653 *A. thaliana*	43029/6.79
29	**5**	1:2.62	*N*-glyceraldehyde 2-phosphotrans-ferase	YFNYYK SQICMVGDR IQPDFYTSK LVFVTNNSTK VYVIGEEGILK IQYGTLCIR ENPGCLFIATNR LIEGVPETLDMLR	gi|8885622 *A. thaliana*	31998/ 5.14
30	**5**	1:3.24	sedoheptulose-bisphos-phatase precursor	MFSPGNLR ATFDNSEYSK FEETLYGTSR GIFTNVTSPTAK TLLMCMGEALR LLFEALQYSHVCK YTGGMVPDVNQIIVK	gi|15228194 *A. thaliana*	42787/6.17
31	**5**	1:2.06	sedoheptulose-bisphos-phatase precursor	TTYVLAVK MFSPGNLR ATFDNSEYSK FEETLYGTSR GIFTNVTSPTAK TLLMCMGEALR LLFEALQYSHVCK YTGGMVPDVNQIIVK	gi|15228194 *A. thaliana*	42787/6.17
32	**5**	1:2.41	glutamine synthetase	AAEIFSNK AILNLSLR DISDAHYK AAEIFSNKK SMREDGGFEVIK TLEKPVEDPSELPK VESLLNLDTKPFTDR IIAEYIWIGGSGIDLR HETASIDQFSWGVANR GGNNILVICDTYTPAGEPIPTNKR WNYDGSSTGQAPGEDSEVILYPQAIFR	gi|12643761 *B. napus*	47714/6.16
33	**5**	1:1.69	ATP synthase β subunit	IGLFGGAGVGK ATNLEMESK AVAMSATEGLK EGNDLYMEMK MPNIYNALVVK AHGGVSVFGGVGER INPTTSDPAVSIR FVQAGSEVSALLGR TVLIMELINNIAK ESGVINELNLADSK VALVYGQMNEPPGAR IVGEEHYETAQQVK IAQIIGPVLDVAFPPGK GIYPAVDPLDSTSTMLQPR GMDVVDMGNPLSVPVGGATLGR DTLGQEINVTCEVQQLLGNNR GRDTLGQEINVTCEVQQLLGNNR GSITSIQAVYVPADDLTDPAPATTFAH LDATTVLSR	gi|8745523 *B. napus*	53740/5.21
34	**6**	1:4.26	rubisco	AVYECLR SQAETGEIK DDENVNSQPFMR	gi|11395 *Cyanophora paradoxa*	53176/6.29
35	**6**	1:2.58	peptidyl-prolyl *cis-trans* isomerase	FEDENFTLK TLESQETR IYACGELPLDA	gi|15228674 *A. thaliana*	28532/8.83
36	**6**	1:4.87	topoisomerase IV subunit B	EERGMGGK	gi|13358029 *Ureaplasma urealyticum*	72719/8.33

Table 3 (Continued)

spot	Figure	quantity ratio of spots[a], sus vs res inoculated	identity	peptides matched	accession no.	M_r/p*I*
37	**6**	1:6.95	CG11450-PA	GTDSADSKPIALVR	gi|17864454 *Drosophila melanogaster*	39869/9.37
38	**6**	1:4.55	rubisco	LNYYTPDYEXK DTDILAAFR	gi|1088276 *Globba curtisii*	50373/7.29
39	**6**	1:8.10	peroxiredoxin type 2	TVTVSSLTAGK	gi|15231718 *A. thaliana*	24783/ 9.12
40	**6**	1:1.51	fructose-bisphosphate aldolase	GILAMDESNATCGK LDSIGLENTEANR TAAYYQQGAR ATPEQVAAYTLK ALQNTCLK ANSLAQLGK YTGEGESEEAK	gi|18420348 *A. thaliana*	43132/6.78

2; **Figure 2**), spot 27 (**Table 3**; **Figure 5**), and spot 40 (**Table 3**; **Figure 6**), both of which were elevated in the resistant genotype after pathogen challenge (**Table 3**), although the level of induction of both spots 27 and 40 was <2-fold. Both of these spots exhibited homology to the same FBPase from *Arabidopsis* (**Table 3**). FBPase is one of the regulatory enzymes of the CO_2 assimilation pathway, and its key position in the Calvin cycle is responsible for the flow of photoassimilated carbon to either starch or sucrose biosynthesis (*28*). Another enzyme with a role in CO_2 assimilation identified in our study as being differentially expressed in the two genotypes is malate dehydrogenase (MDH). MDH acts as a shuttle between the chloroplast and cytosol of photosynthetic cells in the transfer of reducing power between both compartments in C3 plants (*28*). In the present study, malate dehydrogenase (spot 13; **Table 3**; **Figure 4**) appeared to increase in resistant-inoculated plants, although, as with FBPase and TPI, this increase was <2-fold (**Table 3**).

Other than the enzymes directly involved in CO_2 metabolism described above, carbonic anhydrase (CA), which is indirectly related to these pathways, was also identified (spot 6; **Figure 2**) as a unique spot in the resistant genotype. CA catalyzes the reversible hydration of CO_2 and is required for the provision of HCO_3^- for the initial carboxylation reaction catalyzed by phosphoenol pyruvate carboxylase (*29*). It has also been reported that CA is associated with enzymes such as rubisco in the Calvin cycle (*30*) and may provide CO_2 for rubisco. Furthermore, it has been suggested that CA plays an indirect role in photosynthesis by regulating chloroplast pH during rapid changes in light intensity (*31*). CA may also function as a salicylic acid-binding protein and as an antioxidant, thus playing a role in defense responses in tomato as demonstrated by the suppression of the pto:avrpto-mediated hypersensitive response through the silencing of CA gene expression (*32*). Our results provide additional, proteome-level evidence for the role of this relatively uncharacterized enzyme in disease resistance and warrant further investigation.

Increases in the levels of Calvin cycle enzymes such as rubisco, SBPase, TPI, FBPase, and CA suggest the possibility that resistant plants may have a higher photosynthetic efficiency, and this increase in photosynthetic efficiency may contribute to the overall ability of these plants to ward off an infection. Obviously, in susceptible plants the photosynthetic efficiency would be less, particularly in those leaves expressing necrotic symptoms. This is supported by the previously suggested mechanistic basis of disease-induced inhibition of photosynthesis and photosynthetic productivity (*33*). The decrease in the net photosynthetic rate of infected leaves has been attributed to stomatal closure caused by disease-induced water stress, and/or disruption of photosynthesis, including a reduction in the activity of rubisco (*33*, *34*). Our current observations suggest that in the case of resistant plants, such a pathogen-induced inhibition of photosynthesis may not be occurring, which may result in their increased, overall fitness.

Enzymes Involved in Plant Nutrient Metabolism. Glutamine synthetase (GS) is a key enzyme responsible for ammonia assimilation and, in conjunction with glutamate synthase, represents the major pathway for incorporation of ammonia into amino acids (*35*). Overexpression of GS leading to tolerance to abiotic stresses, such as salinity, has been reported and has been attributed to the enhanced scavenging of photorespiratory ammonia (*36*). In *B. napus*, existence of a GS multigene family as well as a well-coordinated and tissue-specific expression of different isoforms of GS during distinct growth phases has been reported (*37*). Our study revealed two GS proteins (spots 4 and 32; **Figures 2** and **5**, respectively). One of them is unique to the susceptible genotype (spot 4; **Table 2**; **Figure 2**); however, it is down-regulated after infection in this genotype (**Figure 2**). The other protein (spot 32; **Figure 5**) common to both genotypes was up-regulated (>2-fold) in resistant plants in response to the pathogen challenge (**Table 3**). GS has been implicated in plant disease including the inhibition of GS activity by the phytotoxin produced by *Pseudomonas syringae* (*38*) as well as in the synthesis of the secondary metabolite camalexin, a phytoalexin demonstrated to be partly responsible for the resistance of *Arabidopsis* to *L. maculans* (*1*, *39*). The precise role of GS in the resistance of the plant material used in our studies needs to be investigated further.

N-Glyceraldehyde-2-phosphotransferase, an enzyme involved in phosphate metabolism, was identified (spot 29; **Table 3**; **Figure 5**) as being elevated in RG plants following pathogen challenge. It has been suggested that phosphatases may be important components of defense responses in plants (*40*). Furthermore, infiltration of potato leaves with the phytopathogenic bacteria *P. syringae* pv. *maculicola* leads to the induction of a phosphate starvation-induced phosphatase gene (*41*). It has been hypothesized that decreased phosphate availability after pathogen infection might act as a signal for the activation of the phosphatase gene. Once again, the increase in the levels (>2-fold; **Table 3**) of *N*-glyceraldehyde-2-phosphotransferase in the resistant plants may indicate the superior ability of this genotype to deal with phosphate deficiencies brought about by the pathogen or to prevent such deficiencies from occurring. As with the other metabolic enzymes identified in this study,

the role of these enzymes in host−pathogen interaction needs to be further characterized.

Enzymes Related to Nitric Oxide (NO) Signaling. Nitrate reductase (NR) is one of the NO-producing enzymes in plants and was identified as unique in the resistant plants (spot 10; **Table 2**; **Figure 2**). NO functions as a signal in plant disease resistance and potentiates the induction of hypersensitive cell death by reactive oxygen intermediates as well as the activation of expression of several defense-related genes (*42*). It has been reported that the activity of NO is dependent and partially required for the functioning of salicylic acid in the systemic acquired resistance signaling pathways in tobacco (*43*). NR is also induced by pathogen signals as reported in potato−*Phytopthora infestans* interaction, where treatment of potato tubers with fungal elicitor hyphal wall components from the fungus induced NR expression at the transcriptional and protein level (*43*). NO increased the synthesis of proteins such as the cyclophilin-type peptidylprolyl isomerases (PPIases), which are involved in the regulation of activity and stability of enzymes (*44*). In this study, we observed two cyclophilin proteins (spots 25 and 35; **Table 3**; **Figures 5** and **6**) in the resistant plants that are up-regulated (**Table 3**) after pathogen challenge. The precise roles of nitrate reductase, nitric oxide, and cyclophilin-type PPIases in this host−pathogen interaction (compatible and incompatible) need to be investigated further and are under study in our laboratory.

Several other proteins of unknown function, including thylakoid luminal protein and a few hypothetical proteins, were identified as up-regulated in resistant plants. Characterizing and understanding the role of these proteins might help to answer several questions regarding both compatible and incompatible *Brassica*−*L. maculans* interaction. It is very interesting to note that no pathogenesis-related proteins or antifungal proteins were identified as being either unique to the resistant genotype or induced in this genotype upon pathogen challenge in our study.

SOD Analysis in Susceptible and Resistant Genotypes. Among the many proteins that were identified in this study as being either unique to the resistant genotype or induced in this genotype in response to the pathogen, the antioxidant enzyme SOD was amenable for further validation due to the availability of spectrophotometric as well as in-gel activity assays. Our spectrophotometric assays for SOD using leaf extracts prepared from pooled plant material from both susceptible and resistant plants revealed significantly higher levels of SOD activity in the resistant plants both prior to and 48 h after pathogen challenge (**Figure 7A**). This is consistent with our proteome-level observation that a unique spot identified as SOD is present in the uninoculated resistant plants, which is also present 48 h after pathogen challenge. We also performed in-gel activity assays for SOD to determine the pattern of SOD isozyme expression in the susceptible and resistant plants. It is evident from **Figure 7B** that at least two additional isozymes are present in the resistant genotype both prior to and 48 h after pathogen challenge. Several SOD isozymes have been reported in plant cells that are differentially regulated according to the need for removal of ROS (*19*). To further validate a role for SOD in pathogen resistance, additional studies aimed at characterizing the detailed expression patterns and activities of the various isozymes of SOD in the resistant and susceptible genotypes are necessary and are in progress in our laboratory.

Global analysis of gene expression through microarrays and ESTs highlights the importance of previously neglected roles of enzymes involved in photosynthetic and other metabolic pathways in disease resistance (*9*, *45*). ESTs of glutamine synthetase, fructose bisphosphate aldolase, triose phosphate isomerase, and carbonic anhydrase along with some PR-proteins have been reported in incompatible *B. napus*−*L. maculans* interaction (*9*). Our current proteome-level investigation using the resistant plants has also revealed some of these proteins in addition to some other metabolic enzymes as well as proteins associated with antioxidant defense responses and NO signaling including PPIase. Although it is possible that the proteome-level changes we are observing might be the downstream effects of a key trigger, additional, detailed studies on the role(s) of selected enzymes identified in this study may provide important clues with respect to their potential involvement in disease susceptibility/resistance. Increasing investigation into the resistance of some varieties of *B. napus* to the blackleg pathogen suggests extremely complex mechanisms and, therefore, it may not be prudent to neglect the possible role of some of the proteins identified in this study. We believe that further in-depth analysis using proteome-level approaches at various stages of pathogen infection as well as the detailed characterization of pathogen-induced gene expression of additional proteins we have identified in this study may reveal potential targets to engineer durable resistance to blackleg disease in *B. napus*.

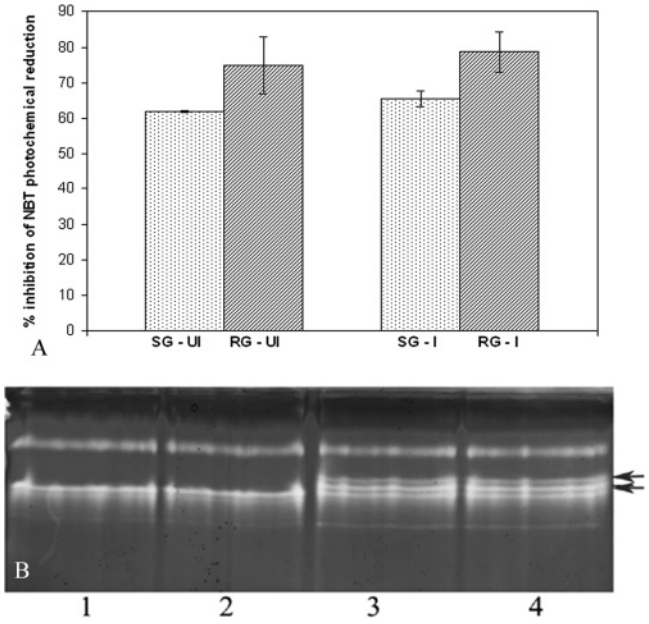

Figure 7. (**A**) SOD activity expressed as percentage inhibition of NBT photochemical reduction. SG-UI, susceptible genotype, uninoculated; RG-UI, resistant genotype, uninoculated; SG-I, susceptible genotype, inoculated; RG-I, resistant genotype, inoculated. (**B**) Isozyme patterns of SOD in susceptible and resistant genotypes 48 h postinoculation: (lane 1) susceptible, uninoculated; (lane 2) susceptible, inoculated; (lane 3) resistant, uninoculated; (lane 4) resistant, inoculated. Arrows indicate the additional isozymes present in the resistant genotype.

ABBREVIATIONS USED

DTT, dithiothreitol; TCA, trichloroacetic acid; IPG, immobilized pH gradient; NBT, nitro blue tetrazolium; rubisco, ribulose bisphosphate carboxylase/oxygenase.

ACKNOWLEDGMENT

We thank Dr. Mike Ellison, Lorne Burke, and Paul Semchuk at the Institute for Biomolecular Design, University of Alberta, for their assistance with mass spectrometry, Dr. Laksiri Goone-

wardane for statistical analysis, and Sanjeeva Srivastava for assistance with the preparation of manuscript.

NOTE ADDED AFTER ASAP PUBLICATION

Species names given incorrectly in the first paragraph under Materials and Methods in the original posting of December 29, 2004, have been corrected in the posting of December 30, 2004.

LITERATURE CITED

(1) Bohman, S.; Staal, J.; Thomma, B. P. H. J.; Wang, M.; Dixelius, C. Characterisation of an *Arabidopsis*−*Leptosphaeria maculans* pathosystem: resistance partially requires camalexin biosynthesis and is independent of salicylic acid, ethylene and jasmonic acid signaling. *Plant J.* **2004**, *37*, 9−20.

(2) Attard, A.; Gout, L.; Gourgues, M. Analysis of molecular markers genetically linked to the *Leptosphaeria maculans* avirulence gene *AvrLm*1 in field populations indicates a highly conserved event leading to virulence on *Rlm*1 genotypes. *Mol. Plant*−*Microbe Interact.* **2002**, *15*, 672−682.

(3) Cozijnsen, A. J.; Popa, K.; Rolls, B. D.; Purwantara, A.; Howlett, B. J. Genome analysis of the plant pathogenic fungus (*Leptosphaeria maculans*); mapping mating type and host specificity loci. *Mol. Plant Pathol.* **2000**, *1*, 293−302.

(4) Chen, C. Y.; Howlett, B. J. Rapid necrosis of guard cells is associated with the arrest of fungal growth in leaves of Indian mustard (*Brassica juncea*) inoculated with avirulent isolates of *Leptosphaeria maculans*. *Physiol. Mol. Plant Pathol.* **1996**, *48*, 73−81.

(5) Roussel, S.; Nicole, M.; Lopez, F.; Ricci, P.;Geige, J.-P.; Renard, M.; Brun, H. *Leptosphaeria maculans* and cryptogein induce similar vascular responses in tissues undergoing the hypersensitive reaction in *Brassica napus. Plant Sci.* **1999**, *144*, 17−28.

(6) Dixelius, C. Presence of the pathogenesis-related proteins 2, Q and S in stressed *Brassica napus* and *Brassica nigra* plantlets. *Physiol. Mol. Plant Pathol.* **1994**, *44*, 1−8.

(7) Rouxel, T.; Kollmann, A.; Boulidard, L.; Mithen, R. Abiotic elicitation of indole phytoalexins and resistance to *Leptosphaeria maculans* within *Brassicaceae*. *Planta* **1991**, *184*, 271−278.

(8) Mahuku, G. S.; Hall, R.; Goodwin, P. H. Co-infection and induction of systemic acquired resistance by weakly and highly virulent isolates of *Leptosphaeria maculans* in oilseed rape. *Physiol. Mol. Plant Pathol.* **1996**, *49*, 61−72.

(9) Fristensky, B.; Balcerzak, M.; He, D.; Zhang, P. Expressed sequence tags from the defense response of *Brassica napus* to *Leptosphaeria maculans*. *Mol. Plant Pathol. Online* **1999**, http://www.bspp.org.uk/mppol/1999/0301.

(10) Rimmer, S. R.; van den Berg, C. G. J. Resistance of oilseed *Brassica* spp to blackleg caused by *Leptosphaeria maculans*. *Can. J. Plant Pathol.* **1992**, *14*, 56−66.

(11) Sacristan, M. D.; Gerdemann, M. Different behaviour of *Brassica juncea* and *Brassica carinata* as sources of *Phoma lingam* resistance in experiments of interspecific transfer to *Brassica napus*. *Z. Pflanzenzuchtg.* **1986**, *97*, 304−314.

(12) Purwantara, A.; Salisbury, P. A.; Burton, W. A.; Howlett, B. J. Reaction of *Brassica juncea* (Indian mustard) lines to Australian isolates of *Leptosphaeria maculans* under glasshouse and field conditions. *Eur. J. Plant Pathol.* **1998**, *104*, 895−902.

(13) Brun, H.; Ruer, D.; Levivier, S.; Somda, I.; Renard, M.; Chevre, A.-M. Presence in *Leptosphaeria maculans* populations of isolates virulent on resistance introgressed into *Brassica napus* from the *B. nigra* B-genome. *Plant Physiol.* **2001**, *50*, 69−74.

(14) Bansal, V. K.; Kharbanda, P. D.; Thiagarajah, M. R.; Tewari, J. P. A comparison of greenhouse and field screening methods for blackleg resistance in doubled haploid lines of *Brassica napus*. *Plant Dis.* **1994**, *78*, 276−281.

(15) Yajima, W.; Hall, J. C.; Kav, N. N. V. Proteome-level differences between auxinic herbicide-susceptible and -resistant wild mustard (*Sinapis arvensis* L.). *J. Agric. Food Chem.* **2004**, *52*, 5063−5070.

(16) Yu, Q.; Rengel, Z. Drought and salinity differentially influence activities of superoxide dismutases in narrow-leafed lupins. *Plant Sci.* **1999**, *142*, 1−11.

(17) El-Moshaty, F. I. B.; Pike, S. M.; Novacky, A. J.; Sehgal, O. P. Lipid peroxidation and superoxide production in cowpea (*Vigna unguiculata*) leaves infected with tobacco ringspot virus or southern bean mosaic virus. *Physiol. Mol. Plant Pathol.* **1993**, *43*, 109−119.

(18) Garcia-Limones, C.; Hervas, A.; Navas-Cortes, J. A.; Jimenez-Diaz, R. M.; Tena, M. Induction of an antioxidant enzyme system and other oxidative stress markers associated with compatible and incompatible interactions between chickpea (*Cicer arietinum* L.) and *Fusarium oxysporum* f.sp. *ciceris. Physiol. Mol. Plant Pathol.* **2002**, *61*, 325−337.

(19) DeGara, L.; dePinto, M. C.; Tommasi, F. The antioxidant systems vis-à-vis reactive oxygen species during plant−pathogen interaction. *Plant Physiol. Biochem.* **2003**, *41*, 863−870.

(20) Morell, S.; Follmann, H.; DeTullio, M.; Haberlein, I. Dehydroascorbate and dehydroascorbate reductase are phantom indictors of oxidative stress in plants. *FEBS Lett.* **1997**, *414*, 567−570.

(21) Wise, R. R. Chilling-enhanced photo oxidation: The production, action and study of reactive oxygen species during chilling in the light. *Photosynthesis Res.* **1995**, *45*, 79−97.

(22) Kingston-Smith, A. H.; Foyer, C. H. Overexpression of Mn-superoxide dismutase in maize leaves leads to increased monodehydroascorbate reductase, dehydroascorbate reductase and glutathione reductase activities. *J. Exp. Bot.* **2000**, *352*, 1867−1877.

(23) Kim, K.; Kim, I. H.; Lee, K.-Y.; Rhee, S. G.; Stadtman, E. R. The isolation and purification of a specific 'protector' protein which inhibits enzyme inactivation by a thiol/Fe(III)/O_2 mixed-function oxidation system. *J. Biol. Chem.* **1988**, *263*, 4704−4711.

(24) Lim, Y. S.; Cha, M.-K.; Uhm, T. B.; Park, J. W.; Kim, K.; Kim. I. H. Removals of hydrogen peroxide and hydroxyl radical by thiol-specific antioxidant protein as a possible role *in vivo*. *Biochem. Biophys. Res. Commun.* **1993**, *192*, 273−280.

(25) Baier, M.; Noctor, G.; Foyer, C. H.; Dietz, K. J. Antisense suppression of 2-cysteine peroxiredoxin in Arabidopsis specifically enhances the activities and expression of enzymes associated with ascorbate metabolism but not glutathione metabolism. *Plant Physiol.* **2000**, *124*, 823−832.

(26) Woodrow, I. E.; Berry, J. A. Enzymic regulation of photosynthetic CO_2 fixation in C3 plants. *Annu. Rev. Plant Physiol. Plant Mol. Biol.* **1988**, *39*, 533−594.

(27) Geiger, D. R.; Servaites, J. C. Diurnal regulation of photosynthetic carbon metabolism in C3 plants. *Annu. Rev. Plant Physiol. Plant Mol. Biol.* **1995**, *45*, 253−256.

(28) Pagano, E. A.; Chueca, A.; Lopez-Gorge, J. Expression of thioredoxins *f* and *m*, and of their targets fructose-1,6-bisphosphatase and NADP-malate dehydrogenase, in pea plants grown under normal and light/temperature stress conditions. *J. Exp. Bot.* **2000**, *51*, 1299−1307.

(29) Hatch, M. D.; Burnell, J. N. Carbonic anhydrase activity in leaves and its role in the first step of C4 photosynthesis. *Plant Physiol.* **1990**, *93*, 380−383.

(30) Jebanathirajah, J. A.; Coleman, J. R. Association of carbonic anhydrase with a Calvin cycle enzyme complex in *Nicotiana tabacum. Planta* **1998**, *204*, 177−182.

(31) Reed, M. L.; Graham, D. Carbonic anhydrase in plants: distribution, properties and possible physiological roles. *Prog. Phytochem.* **1981**, *7*, 47−94.

(32) Slaymaker, D. H.; Navarre, D. A.; Clark, D.; del Pozo, O.; Martin, G. B.; Klessig, F. The tobacco salicylic acid-binding protein 3 (SABP3) is the chloroplastic carbonic anhydrase, which exhibits antioxidant activity and plays a role in the hypersensitive defence response. *Proc. Natl. Acad. Sci. U.S.A.* **2002**, *99*, 11640−11645.

(33) Nogues, S.; Cotxarrera, L.; Alegre, L.; Trillas, M. I. Limitations to photosynthesis in tomato leaves induced by *Fusarium* wilt. *New Phytol.* **2002**, *154*, 461−470.

(34) Santos, L.; Lucio, J.; Odair, J.; Carneiro, M. L.; Alberto, C. Symptomless infection of banana and maize by endophytic fungi impairs photosynthetic efficiency. *New Phytol.* **2000**, *147*, 609−615.

(35) Fei, H.; Chaillou, S.; Hirel, B.; Mahon, J. D.; Vessey, J. K. Overexpression of a soybean cytosolic glutamine synthetase gene linked to organ-specific promoters in pea plants grown in different concentrations of nitrate. *Planta* **2003**, *216*, 467−474.

(36) Hoshida, H.; Tanaka, Y.; Hibino, T.; Hayashi, Y.; Tanaka, A.; Takabe, T.; Takabe, T. Enhanced tolerance to salt stress in transgenic rice that overexpresses chloroplast glutamine synthetase. *Plant Mol. Biol.* **2000**, *43*, 103−111.

(37) Ochs, G.; Schock, G.; Trischler, M.; Kosemund, K.; Wild, A. Complexity and expression of the glutamine synthetase multigene family in the amphidiploid crop *Brassica napus. Plant Mol. Biol.* **1999**, *39*, 395−405.

(38) Langston-Unkefer, P. J.; Robinson, A. C.; Knight, T. J.; Durbin, R. D. Inactivation of pea seed glutamine synthetase by the toxin, tabtoxinine-β-lactam. *J. Biol. Chem.* **1987**, *262*, 1608−1613.

(39) Zhao, J.; Williams, C. C.; Last, R. L. Induction of *Arabidopsis* tryptophan pathway enzymes and camalexin by amino acid starvation, oxidative stress, and an abiotic elicitor. *Plant Cell* **1998**, *10*, 359−370.

(40) Rodriguez, P. L. Protein phosphatase 2C (PP2C) function in higher plants. *Plant Mol. Biol.* **1998**, *38*, 919−927.

(41) Petters, J.; Gobel, C.; Scheel, D.; Rosahl, S. A pathogen-responsive cDNA from potato encodes a protein with homology to a phosphate starvation-induced phosphatase. *Plant Cell Physiol.* **2002**, *43*, 1049−1053.

(42) Delledonne, M.; Xia, Y.; Dixon, R. A.; Lamb, C. Nitric oxide functions as a signal in plant disease resistance. *Nature* **1998**, *394*, 585−588.

(43) Yamamoto, A.; Katou, S.; Yoshioka, H.; Doke, N.; Kawakita, K. Nitrate reductase, a nitric oxide-producing enzyme: induction by pathogen signals. *J. Gen. Plant Pathol.* **2003**, *69*, 218−229.

(44) Morot-Gaudry-Talarmain, Y.; Rockel, P.; Moureaux, T.; Quilleré, I.; Leydecker, M.; Kaiser, W.; Morot-Gaudry, J. Nitrate accumulation and nitric oxide emission in relation to cellular signaling in nitrite reductase antisense tobacco. *Planta* **2002**, *215*, 708−715.

(45) Rao, Z. M.; Dong, H. T.; Zhuang, J. Y.; Chai, R. Y.; Fan. Y. Y.; Li, D. B.; Zheng, K. L. Analysis of gene expression profiles during host-*Magnaporthe grisea* interactions in a pair of near isogenic lines of rice. *Yi Chuan Xue Bao* **2002**, *29*, 887−893.

Received for review June 30, 2004. Accepted October 13, 2004. Financial assistance from the Natural Sciences and Engineering Research Council of Canada (NSERC), Alberta Agricultural Research Institute (AARI), and Alberta Crop Industry Development Fund (ACIDF) is gratefully acknowledged.

JF048922Z